

Landau quantization effects in the charge-density-wave system $(\text{Per})_2M(\text{mnt})_2$ (where $M = \text{Au}$ and Pt)

R. D. McDonald¹, N. Harrison¹, J. Singleton¹, A. Bangura², P.A. Goddard¹, A. P. Ramirez³ and X. Chi³

¹*National High Magnetic Field Laboratory, LANL, MS-E536, Los Alamos, New Mexico 87545*

²*The Clarendon Laboratory, Parks Road, Oxford OX1 3PU, United Kingdom*

³*Bell Laboratories, Lucent Technologies, 600 Mountain Avenue, Murray Hill, New Jersey 07974*

(Dated: May 31, 2018)

A finite transfer integral t_a orthogonal to the conducting chains of a highly one-dimensional metal gives rise to empty and filled bands that simulate an indirect-gap semiconductor upon formation of a commensurate charge-density-wave (CDW). In contrast to semiconductors such as Ge and Si with bandgaps ~ 1 eV, the CDW system possesses an indirect gap with a greatly reduced energy scale, enabling moderate laboratory magnetic fields to have a major effect. The consequent variation of the thermodynamic gap with magnetic field due to Zeeman splitting and Landau quantization enables the electronic bandstructure parameters (transfer integrals, Fermi velocity) to be determined accurately. These parameters reveal the orbital quantization limit to be reached at ~ 20 T in $(\text{Per})_2M(\text{mnt})_2$ salts, making them highly unlikely candidates for a recently-proposed cascade of field-induced charge-density wave states.

PACS numbers: 71.45.Lr, 71.20.Ps, 71.18.+y

Magnetic fields B affect the energies of band electrons via Landau (orbital) quantization and Zeeman (spin) splitting [1]. In semiconductors such as GaAs and Si, the characteristic energies of these effects for $B \lesssim 100$ T are much smaller than the energy gap, E_g , and the conduction- and valence-band widths, all of which are ~ 1 eV; hence, the field can be regarded as a mere perturbation of the overall bandstructure. By contrast, commensurate charge-density wave (CDW) groundstates have the potential to provide analogues in which E_g and the bandwidths are scaled down by factors $\sim 10 - 1000$ [2]. An ‘‘indirect-gap semiconductor’’ is produced in a CDW if the characteristic bandwidth $4t_a$ of the electronic dispersion orthogonal to the chain direction (and nesting vector \mathbf{Q}) is comparable to but smaller than the order parameter 2Δ (see Fig. 1 b). In such circumstances, the small size of E_g means that the Landau and Zeeman energies due to typical laboratory fields are major effects, resulting in marked alterations to the overall electronic properties.

In this Letter, we show that CDW materials of the composition $(\text{Per})_2M(\text{mnt})_2$, with $M = \text{Au}$ and Pt , are ideal candidates for this purpose [3]. Fields of $B < 45$ T have been shown to suppress the CDW groundstates of these systems [4, 5, 6, 7], providing an estimate for 2Δ of a few meV, only slightly larger than the $4t_a \sim 1$ meV obtained from bandstructure calculations [8]. Landau quantization and Zeeman splitting of the filled and empty states (Fig. 1d) leads to a field-dependent thermodynamic energy gap $E_g(B)$, that may, with care, be extracted from the thermally-activated component of the conductivity

$$\sigma_T = \sigma_0 \exp[-E_g(B)/2k_B T], \quad (1)$$

where T is the temperature. The measured $E_g(B)$ provides a means of deducing both $4t_a$ and the Fermi velocity v_F along the chains. These values are consistent with bandstructure calculations [8] and are in good agreement

with estimates from thermopower data [3]. The data also enable us to identify the maximum field at which closed orbits can exist, which is found to be too small to support recently-postulated field-induced charge-density wave states in $(\text{Per})_2M(\text{mnt})_2$ salts [6].

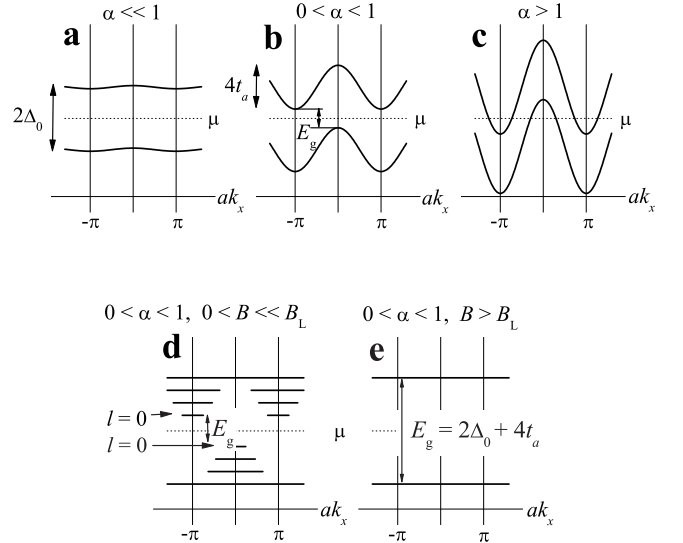


FIG. 1: Electronic dispersion at $k'_y = 0$ according to Eq. 5 for differing values of $\alpha = 2t_a/\Delta$: **a**: $\alpha \ll 1$, **b**: $0 < \alpha < 1$, **c**: $\alpha > 1$. Scenario **b** corresponds to an indirect gap semiconductor. **d**: Schematic of the Landau quantization of scenario **b** in the presence of finite B (ignoring the Zeeman effect, for clarity). **e**: The gap beyond the field limit for Landau quantization ($B > B_L$; see text). In all diagrams, μ represents the chemical potential.

Charge transfer between $(\text{Per})_2^+$ and $M(\text{mnt})_2^-$ in $(\text{Per})_2M(\text{mnt})_2$ gives rise to a normal metallic state with a highly one-dimensional (1D) $3/4$ -filled band in which v_F is directed along the Perylene chains parallel to the

crystallographic \mathbf{b} axis [8]. Commensurate CDW ground-states occur for $M = \text{Pt}$, Cu and Au , in which the 1D band becomes gapped upon modulation of the lattice at a postulated [9] wavevector $\mathbf{Q} = (0, 2k_F, 0)$, where $\pm k_F = \frac{\pi}{4}|\mathbf{b}|$ [10]. Transitions into the CDW ground-state occur at $T_P \approx 12$ K for $M = \text{Au}$ and $T_P \approx 8$ K for $M = \text{Pt}$. In the case of $M = \text{Pt}$, this is accompanied by the synchronous dimerization of the $S = 1/2$ Pt spins [10]: we return to the special case of $M = \text{Pt}$ below. In all cases, semiconducting behaviour occurs for $T \leq T_P$; as T is reduced further, in addition to the thermally-activated conduction, there is an increasing contribution from the sliding collective mode of the CDW as a characteristic threshold electric field \mathcal{E}_t is approached [5].

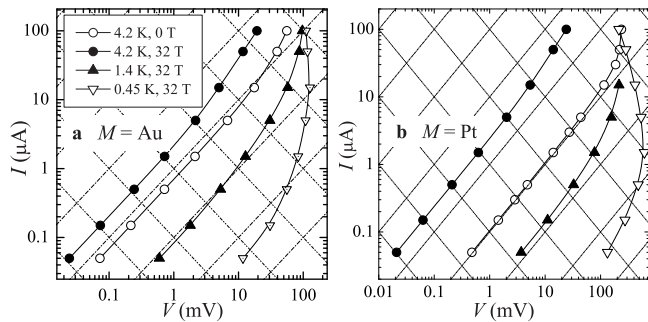


FIG. 2: Non-linear current-versus-voltage characteristics of $(\text{Per})_2\text{Au}(\text{mnt})_2$ (a) and $(\text{Per})_2\text{Pt}(\text{mnt})_2$ (b) plotted on logarithmic scales for various temperatures and fields (see inset key). The negative-slope diagonal lines are contours of constant power and the positive-slope diagonal lines are contours of constant resistance, providing a guide as to when the sample's behavior is dominated by ohmic, thermally-activated conduction rather than sliding.

In these experiments, $E_g(B)$ is determined for $M = \text{Au}$ and Pt using transport measurements in static fields of up to 33 T, with $0.45 \text{ K} \leq T \leq 4.2 \text{ K}$ provided by a ^3He cryostat. Currents as low as $I = 50 \text{ nA}$ (equivalent to a current density $j_y \approx 50 \text{ Am}^{-2}$) applied along the crystal's b direction, enable E_g to be extracted from the T -dependence of the resistance R (proportional to the resistivity tensor component ρ_{yy} [7]) over a range of T where the contribution from the CDW collective mode is small. Figure 2 shows that this is the case over a wide range of B provided $I \lesssim 100 \text{ nA}$ and $T \gtrsim 1 \text{ K}$.

Figures 3a and b show examples of Arrhenius plots of the resistance R versus reciprocal temperature $1/T$ for $M = \text{Au}$ and Pt respectively, made using $I = 50 \text{ nA}$ with $\mathbf{B} \parallel \mathbf{c}^*$ at several different B . Prior studies [5, 7] have shown that ρ_{yy} in $(\text{Per})_2M(\text{mnt})_2$ conforms to a simple parallel conduction model in which the Hall component of the conductivity tensor $\sigma_{xy} \approx 0$, leading to

$$\rho_{yy} = (\sigma_T + j_y/\mathcal{E}_t)^{-1}, \quad (2)$$

where j_y/\mathcal{E}_t is the contribution from the collective mode. As discussed below, the expression for $E_g(B)$ (Eq. 7) contains Δ , which is T -dependent; moreover, \mathcal{E}_t may depend

on T . Thus, the slope of an Arrhenius plot becomes

$$\frac{\partial \ln \rho_{yy}}{\partial(1/T)} = \frac{\frac{1}{2k_B}(E_g - T \frac{\partial E_g}{\partial T}) - \frac{2k_B j_y T^2}{\sigma_T \mathcal{E}_t^2} \frac{\partial \mathcal{E}_t}{\partial T}}{1 + \frac{j_y}{\sigma_T \mathcal{E}_t}}. \quad (3)$$

Since \mathcal{E}_t is expected to depend strongly on T only as $T \rightarrow T_P$ [11], the last term on the right-hand-side of Eq. 3 should be negligible for $T \lesssim T_P/2$ and sufficiently small j_y . The second term can also be minimized by evaluating the slope for $T < T_P/2$; using a mean-field expression for $\Delta(T)$ [2], these conditions give $-2T \partial E_g / \partial T \equiv -T \partial \Delta / \partial T < 0.1 \Delta$. In the present case, we choose $T \approx T_P/3$, such that $-T \partial \Delta / \partial T \approx 0.05 \Delta$, yielding $\partial \ln(\rho_{yy}) / \partial(1/T) \approx E_g / 2k_B$ with a systematic error of only $\sim 5\%$. In using this method to extract E_g , it is important to note that $T_P = T_P(B)$ [4]; thus, the exact T range used depends on the applied field.

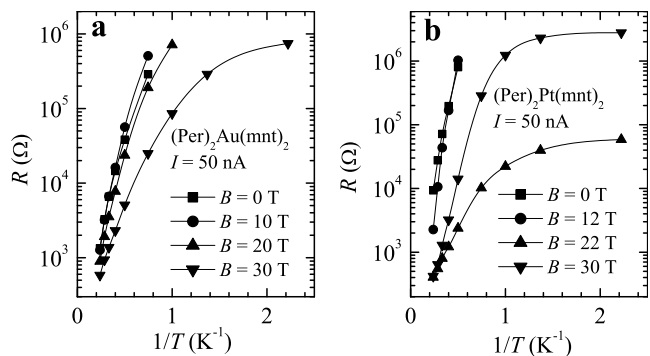


FIG. 3: Arrhenius plots of R (logarithmic scale) versus $1/T$ with $I = 50 \text{ nA}$ for (a) $M = \text{Au}$ and (b) $M = \text{Pt}$ at several different magnetic field strengths B .

At lower T , the number of thermally-activated carriers decreases significantly, rendering their contribution to the conductivity negligible. The consequent larger potential difference across the sample results in increased depinning of the CDW, so that $\ln(R)$ saturates at lower T (i.e. higher $1/T$) in Fig. 3. As shown in Fig. 2, the point at which significant CDW depinning occurs is shifted to lower T (higher $1/T$) by the use of small currents.

By using larger currents of 1 and 10 μA , Graf *et al* [4] obtained an Arrhenius plot in which the CDW was highly depinned over an extensive range of T , causing $\ln(\rho_{yy})$ versus $1/T$ to exhibit significant curvature even at $T \sim T_P/3$. To make matters worse, Graf *et al.* extracted $\partial \rho_{yy} / \partial(1/T)$ at $T \approx 0.7 T_P$, at which $-T \partial \Delta / \partial T > \Delta$. Sadly, these factors introduced a systematic error $\sim 100\%$, resulting in an overestimate of E_g by a factor ~ 2 .

The present estimate of $E_g \approx 3.2 \text{ meV}$ made at $T \approx T_P/3$ and $B = 0$ with $I = 50 \text{ nA}$, shown in Fig. 4a, is rather less than the value of $2\Delta_0 \approx 4.5 \text{ meV}$ deduced for $M = \text{Au}$ from its Pauli paramagnetic limit [5], supporting the scenario depicted in Fig. 1b. This can be modeled using a simplified dispersion of the form

$$\varepsilon = -2t_a \cos ak_x - \hbar v_F |k_y - k_F|, \quad (4)$$

where $v_F = \sqrt{2}bt_b/\hbar$ is the magnitude of \mathbf{v}_F directed along \mathbf{b} for a $\frac{3}{4}$ -filled band. Here, t_a , t_b , a (≈ 17 Å) and b (≈ 4.2 Å) are the transfer integrals and lattice spacings perpendicular and parallel to the chains respectively. On opening a gap 2Δ (which may be smaller than $2\Delta_0$ at finite T), the dispersion becomes [11]

$$\varepsilon_g = -2t_a \cos ak_x \pm \sqrt{(\hbar v_F k'_y)^2 + \Delta^2}, \quad (5)$$

where we have substituted $k'_y = k_y - k_F$ for clarity. At $k'_y = 0$, the electronic dispersion versus k_x consists of a pair of narrow bands above and below μ , separated in energy by 2Δ , as shown in Fig. 1 for different values of $\alpha = 2t_a/\Delta$. When $\alpha \ll 1$, one obtains a gap with little dispersion. This is the likely scenario for CDW materials with very large order parameters such as $(\text{TaSe}_4)_2\text{I}$ or TaS_3 [2]. In the opposite extreme, $\alpha > 1$, one obtains a semimetal qualitatively similar to NbSe_3 [2] or perhaps α -(BEDT-TTF) $_2\text{MHg}(\text{SCN})_2$, in which field-induced CDW phases have been suggested [12]. An indirect gap semiconductor with $E_g = 2\Delta - 4t_b$ between filled and empty states separated by the vector $[\pi/a, 0]$ is obtained for the intermediate situation where $0 < \alpha < 1$.

The introduction of finite B has two effects on Eq. 5. The first is to Zeeman split the two bands into four subbands with energies

$$\varepsilon_g = -2t_a \cos ak_x \pm \sqrt{(\hbar v_F k'_y)^2 + \Delta^2} + gs\mu_B B, \quad (6)$$

where s ($= \pm \frac{1}{2}$) is the electron spin and g (≈ 2) is its Landé g-factor. Thus, the smallest (*thermodynamic*) gap occurs between the maximum of the $s = +\frac{1}{2}$ subband below μ and the minimum of the $s = -\frac{1}{2}$ subband above μ , yielding $E_g = 2\Delta - 4t_a - g\mu_B B$. The second effect of finite B is to quantize the orbital motion of the empty and filled states immediately above and below the gap, giving rise to sets of completely empty and filled Landau levels at $T = 0$ (Fig. 1d). At finite T , carrier excitations occur between the $l = 0$ Landau levels on either side of μ , leading to a thermodynamic gap

$$E_g(B) = 2\Delta - 4t_a - g\mu_B B + \gamma \hbar \omega_c \quad (7)$$

where $\omega_c = eB/m^*$ is the magnitude of the cyclotron frequency of the $l = 0$ Landau level of the two relevant subbands in the limit $B \rightarrow 0$ and m^* is an effective mass, to be defined below.

The parameter γ describes the (identical) nonparabolicities of the $s = +\frac{1}{2}$ subband below μ and the $s = -\frac{1}{2}$ subband above μ ; it is derived by equating the k -space area $A_k(\varepsilon_g)$ of an orbit of constant energy ε_g (from Eq. 6) with the Onsager k -space area $A_{l=0} = \pi eB/\hbar$ of the $l = 0$ Landau level [1]. This cannot be done analytically; instead, the fit (solid line) to the data in Fig. 4a for $M = \text{Au}$ incorporates a numerical integration $A_k(\varepsilon_g) = \int \Theta|\varepsilon_g| dk_x dk'_y$, where Θ is the theta function (*i.e.* the integral of the Kronecker δ).

The fit involves adjusting three parameters, 2Δ , $4t_a$ and v_F . A satisfactory fit is obtained for $M = \text{Au}$ using

$4t_a = 0.80 \pm 0.03$ meV, $v_F = (1.70 \pm 0.05) \times 10^5$ ms $^{-1}$ and $2\Delta = 4.02 \pm 0.03$ meV; note that over the T range used, the deduced value of Δ is equal to Δ_0 to a good approximation. These parameters correspond to $E_g = 3.21 \pm 0.03$ meV at $B = 0$, $T = 0$ and an intrachain bandwidth of $4t_b \approx 752$ meV; the latter value is very close to estimates from thermopower data ($4t_a \approx 740$ meV) [3] and in reasonable accord with bandstructure calculations ($4t_a \approx 590$ meV) [8].

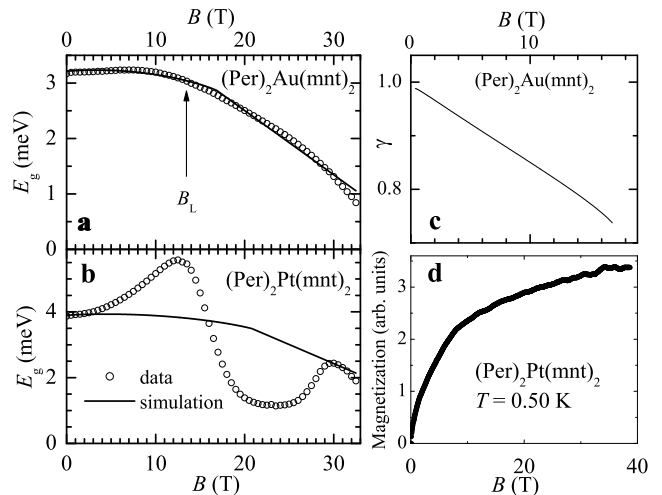


FIG. 4: The excitation gap E_g (circles) for $M = \text{Au}$ (a) and $M = \text{Pt}$ (b) estimated from the slopes of Arrhenius plots like those in Fig. 3 at $T \approx T_P/3$ at many different values of the applied B . The solid lines represent fits of the model described in the text. (c) The parameter $\gamma(B)$ obtained by fitting the experimentally-estimated gap in a. (d) Magnetization of many randomly-orientated $M = \text{Pt}$ crystals at $T = 0.50$ K measured using an extraction magnetometer in a pulsed magnetic field [14].

Figure 4c shows the field dependence of γ in Eq. 7. At $B = 0$, $\gamma = 1$ due to the approximately parabolic curvature of the bands close to their extrema

$$\varepsilon_g \approx 2\Delta - 4t_a \pm g\mu_B B + \frac{\hbar^2 k_x^2}{2m_a} + \frac{\hbar^2 k_y^2}{2m_\Delta} + \dots \quad (8)$$

Here, $m^* = 0.90m_e$ is an effective mass (m_e is the free electron mass), given by $m^* = \sqrt{m_a m_\Delta}$ for an approximately elliptical orbit where $m_a = \hbar^2/2a^2 t_a \approx 50 m_e$ and $m_\Delta = \Delta/v_F^2 \approx 0.01 m_e$. Eq. 7 therefore describes a situation in which E_g initially increases with B at a rate $\partial E_g/\partial B \approx \hbar e(m_e - m^*)/m^* m_e$, owing to the fact that $m^* < m_e$ and $g\mu_B \approx \hbar e/m_e$. As B increases further, the nonparabolic curvature of Eq. 6 at $|\varepsilon_g| > \Delta - 2t_a - g\mu_B B$ eventually causes E_g to fall, corresponding to a reduction in γ in Fig. 4 (inset). This occurs until the $l = 0$ Landau level of each subband acquires an energy of magnitude $|\varepsilon_g(B)| = |(\Delta + 2t_a - g\mu_B B_L)|$ at the limit

$$B_L = 8t_a m^*/\gamma \hbar e, \quad (9)$$

at which $\gamma\hbar\omega_c = 8t_a$, $k_x = \pi/a$ and closed orbits can no longer exist. This limit corresponds to the largest possible pocket created by imperfect nesting matching the k -space area $A_{l=0} \approx 10^{17} \text{ m}^{-2}$ ($\approx 0.15\%$ of the Brillouin zone) of the $l = 0$ Landau level. Orbitally-quantized states can therefore not exist in $(\text{Per})_2\text{Au}(\text{mnt})_2$ at fields greater than 17 T, supporting the existence of an inhomogeneous CDW phase in this material at $B \gtrsim 30 \text{ T}$ [7] as opposed to a cascade of field-induced CDW states involving orbital quantization [12, 13]. The absence of Landau subbands for $B \geq B_L \approx 17 \text{ T}$ ($M=\text{Au}$) leads to a simpler field-dependent gap

$$E_g = 2\Delta + 4t_a - g\mu_B B. \quad (10)$$

The slope for $B > B_L$ is determined entirely by $|gs| \approx 1$, making it independent of all fitting parameters. Only the intercept of Eq. 10 at $B = 0$ is determined by $2\Delta + 4t_a$. Hence, the portion of the fit for $B > B_L$ in Fig. 4a effectively involves the adjustment of only a single parameter, imposing a severe constraint on $2\Delta + 4t_a$ and thereby adding further confidence in the model.

For $M = \text{Au}$, we have shown that a uniform CDW order parameter $2\Delta_0 \approx 2\Delta = 4.02 \pm 0.03 \text{ meV}$, bandwidth $4t_a = 0.80 \pm 0.03 \text{ meV}$ and Fermi velocity $v_F = (1.70 \pm 0.05) \times 10^5 \text{ ms}^{-1}$ explain the experimentally-observed field-dependence of E_g . This requires a revision of our estimate for the Pauli paramagnetic limit to $B_P = (\Delta_0 + 2t_a)/\sqrt{2}gs\mu_B \approx 30 \text{ T}$, which now approximately corresponds to the field at which \mathcal{E}_t starts to drop experimentally [5]. The revised estimate of $2\Delta_0$ further yields $\zeta = k_B T_P / 2\Delta_0 \approx 3.9$: since this estimate only marginally exceeds the BCS value of $\zeta = 3.52$, it implies that the CDW groundstate of $(\text{Per})_2M(\text{mnt})_2$ with $M = \text{Au}$ is weakly coupled to the crystalline lattice [2].

Turning now to the case of $M = \text{Pt}$, it is clear that E_g is larger at $B = 0$, in spite of the lower T_p ($\approx 8 \text{ K}$). The complex field-dependent behavior that takes place for $3 < B < 30 \text{ T}$ only in the case of $M = \text{Pt}$ must be the

consequence of interactions involving the dimerization of the $S = 1/2$ Pt spins, which are not included in the present simulation. In situations in which the magnetization (Fig. 4d) is either small ($B \approx 0$) or approaching saturation ($B \approx 30 \text{ T}$), the use of $4t_a = 1 \text{ meV}$ and the same v_F as in $M = \text{Au}$ results in a fitted value $2\Delta \approx 4.8 \text{ meV}$. In the absence of a more sophisticated model, one can conclude from the estimate of $\zeta = 2\Delta_0/k_B T_P \approx 7$, that the dimerization of the Pt spins in $(\text{Per})_2\text{Pt}(\text{mnt})_2$ causes the CDW groundstate to be more strongly coupled to the crystalline lattice than in the case of $M = \text{Au}$. The consequent larger lattice distortion in $M = \text{Pt}$ might explain its higher \mathcal{E}_t values compared to those of $M = \text{Au}$ (Fig. 2). It may also be the reason why X-ray Bragg reflection peaks due to dimerization have been seen for $M = \text{Pt}$ but not for $M = \text{Au}$ [3].

In conclusion, $(\text{Per})_2\text{Au}(\text{mnt})_2$ is shown to possess an ideal combination of parameters for modeling the effect of a strong magnetic field on an indirect gap semiconductor. A model that includes the effect of Zeeman splitting and Landau quantization of subbands with a conventional field-independent order parameter (for fields below the Pauli paramagnetic limit) provides a good description of the experimental data [15]. The electronic structure parameters obtained reveal the limiting magnetic field for closed orbits to be $B_L \approx 17 \text{ T}$, implying field-induced CDW states that incorporate orbitally quantized levels cannot exist at $B \gtrsim 17 \text{ T}$ in $(\text{Per})_2\text{Au}(\text{mnt})_2$. The electronic structure of $(\text{Per})_2\text{Pt}(\text{mnt})_2$ is expected to be similar. However, the existence of $S = 1/2$ Pt spins causes a stronger coupling of the CDW to the lattice followed by a more complex dependence of E_g on field for $B \lesssim 30 \text{ T}$ that has yet to be modeled.

This work is supported by US Department of Energy (DOE) grants LDRD20030084DR and LDRD2004009ER and was performed under the auspices of the National Science Foundation, the DOE and the State of Florida. We thank Chuck Mielke and Albert Migliori for very useful comments.

-
- [1] N. W. Ashcroft and N. D. Mermin, *Solid State Physics* (Saunders College Publishing, 1976).
 - [2] G. Grüner, *Density waves in solids, Frontiers in physics* **89** (Addison-Wesley, 1994).
 - [3] R. T. Henriques *et al.*, J. Phys. C: Solid State Phys. **17**, 5197 (1984).
 - [4] D. Graf *et al.*, Phys. Rev. B **69**, 125113 (2004).
 - [5] R. D. McDonald *et al.*, Phys. Rev. Lett. **93**, 076405 (2004).
 - [6] D. Graf *et al.*, Phys. Rev. Lett. **93**, 076406 (2004).
 - [7] R. D. McDonald *et al.*, cond-mat/0408408.
 - [8] L. F. Veiros *et al.*, Inorg. Chem. **33**, 4290 (1994).
 - [9] V. Gama *et al.*, Synth. Metals **55-57**, 1677 (1993).
 - [10] E. B. Lopes *et al.*, J. Phys. I France **6**, 2141 (1996).
 - [11] B. Korin-Hamzić *et al.*, Europhysics Lett. **59**, 298 (2002).
 - [12] D. Andres *et al.*, Phys. Rev. B **68**, 201101 (2003).
 - [13] A. G. Lebed, JETP Letters **78**, 170 (2003).
 - [14] P.A. Goddard *et al.*, to be published.
 - [15] A similar model has been applied successfully to the spin-density-wave state of $(\text{TMTSF})_2\text{PF}_6$, for which Zeeman effects are absent [11]. We are grateful to Kazumi Maki for pointing this work out to us.